

EFFECTS OF WAKE AND BOUNDARY LAYER INTERACTION ON NOISE SOURCES FOR A MODEL AIRFRAME PROBLEM

William R. Wolf¹, Bruno Backes², Edemar Morsch Filho², João Luiz F. Azevedo*³

¹Universidade Estadual de Campinas, UNICAMP, Campinas, SP, 13083-970, Brazil
wolf@fem.unicamp.br

²Universidade Federal de Santa Catarina, UFSC, Joinville, SC, 89218-000, Brazil
{bbackesbruno,ede.morsch}@gmail.com

³Instituto de Aeronáutica e Espaço, DCTA/IAE/ALA, São José dos Campos, SP, 12228-903, Brazil
joaoluiz.azevedo@gmail.com

Keywords: Aeroacoustics, Airframe Noise, Quadrupole Source Terms, Convective Effects, Wake Interactions, Boundary Layer Interactions.

Abstract. *In practical predictions of low and moderate Mach number airframe noise, the large disparity in energy scales between the hydrodynamic and acoustic fields makes it impractical to directly compute far field noise. Hybrid methods have been widely used as a solution to this problem where the source field is computed separately from the acoustic field using an acoustic analogy. Typically, the analogy is derived from Lighthill's work, with the Ffowcs Williams-Hawkings (FW-H) formulation commonly used in airframe noise problems. The analogy includes contributions from sources integrated along the geometric surfaces (monopoles and dipoles) as well as volumetric sources along boundary layer and wake regions (quadrupoles). Due to the cost of computing the volume integrals, quadrupole terms are often neglected. However, recent studies have shown that, even at moderate Mach numbers, quadrupole sources can have a non-negligible effect on far field acoustic predictions. It has also been demonstrated that quadrupole sources have a significant impact on predictions involving airframe configurations, particularly those with wake interactions. In the present work, direct noise calculations of a model airframe noise problem are conducted in order to assess the effects of wake and boundary layer interaction on aeroacoustics. Simulations of unsteady laminar flows including both noise generation, and its subsequent propagation to the far field, are performed for a 2-D configuration composed of a cylinder placed above a NACA 0012 airfoil at 5 deg. angle of attack. The Reynolds number based on the airfoil chord is 5000 and that based on the diameter of the cylinder is 200. An assessment of cylinder position and freestream Mach number effects on sound radiation is presented. An assessment of the noise sources is discussed using a hybrid methodology which employs direct calculation for nearfield source computations and the FW-H equation as the acoustic analogy formulation. The integrations of surface dipole and volume quadrupole source terms in the FW-H formulation are accelerated by a wideband multi-level adaptive fast multipole method that incorporates convective effects.*

1 INTRODUCTION

In practical problems of interest, especially the prediction of low and moderate Mach number airframe noise, the large disparity in energy scales between the hydrodynamic and acoustic fields makes it impractical to directly compute far field noise. Hybrid methods have been widely utilized as a solution to this problem where the source field is computed separately from the acoustic field using an acoustic analogy. Typically, the analogy is derived from Lighthill's work [1], with the Ffowcs Williams-Hawkings [2] (FW-H) formulation commonly used in airframe noise problems. The analogy includes contributions from sources integrated along the geometry surfaces (monopoles and dipoles) as well as volumetric sources along boundary layer and wake regions (quadrupoles). Due to the cost of computing the volume integrals, quadrupole terms are often neglected. In low Mach number flows, this approximation should be reasonable since the effects of quadrupoles are small relative to the effects of dipoles and monopoles. However, recent studies have shown that, at moderate Mach numbers, quadrupole sources can have a non-negligible effect on far field acoustic predictions [3, 4]. Additionally, it has been demonstrated that quadrupole sources have a significant impact on predictions involving airframe configurations, particularly those with wake interactions.

With growing interest in noise predictions of complex airframe configurations, the issue of quadrupole noise is of paramount importance. At flight Reynolds numbers, turbulent wakes form and interact downstream of the geometries studied. In these cases, it is unclear when quadrupoles may play an important role and when they may be neglected. Casper *et al.* [5] showed that the inclusion of quadrupole terms was necessary for accurate predictions of a multi-element airfoil at $M_\infty = 0.2$. Spalart *et al.* [6] found evidence to suggest that quadrupole noise for a simple landing gear array may still be significant at $M_\infty = 0.115$. Recently, Wolf *et al.* [7] presented results for a NACA 0012 airfoil at $M_\infty = 0.4$ showing that quadrupole effects become non-negligible at medium and high frequencies. The previous authors also demonstrated in Ref. [8] that volumetric sources can add up to ≈ 4 dB in OASPL at upstream observer angles.

In the present work, aeroacoustic predictions of a two-dimensional model airframe noise problem are conducted in order to assess the effects of wake and boundary layer interaction on both the near flow field and acoustic field. Although simulations are performed using a two-dimensional formulation, several aerodynamic and aeroacoustic physical mechanisms are also found in three-dimensional computations of similar configurations [9]. Simulations of unsteady laminar flows including both noise generation, and its subsequent propagation to the far field, are performed for a two-dimensional configuration composed of a cylinder placed above a NACA 0012 airfoil at 5 deg. angle of incidence. The Reynolds number based on the airfoil chord is $Re_c = 5000$ and the Reynolds number based on the diameter of the cylinder is $Re_d = 200$. An assessment of cylinder position and freestream Mach number effects on sound radiation is presented for $M_\infty = 0.1, 0.3$ and 0.5 . The investigation of the noise sources for airfoil and cylinder vortex shedding frequencies is also presented using a hybrid methodology which employs direct noise calculation (DNC) for near field source computations and the Ffowcs Williams-Hawkings (FW-H) equation as the acoustic analogy formulation. The integrations of surface dipole and volume quadrupole source terms appearing in the FW-H formulation are accelerated by a fast multipole method [3] that incorporates convective effects. In order to verify the numerical solutions, acoustic prediction results obtained by direct noise calculation (DNC) are compared to those computed by the FW-H equation and good agreement is observed.

2 FLOW SIMULATIONS

The general curvilinear form of the compressible Navier-Stokes equations is solved in conservation form. The numerical scheme for spatial discretization is a sixth-order accurate compact scheme [10] implemented on a staggered grid. The current numerical capability allows the use of overset grids with a fourth-order accurate Hermite interpolation between grid blocks [11]. Compact finite-difference schemes are non-dissipative and numerical instabilities arising from insufficient grid resolution, mesh non-uniformities, approximate boundary conditions and interpolation at grid interfaces have to be filtered to preserve stability of the numerical schemes. The high wavenumber compact filter presented by Lele [12] is applied to the computed solution at prescribed time intervals in order to control numerical instabilities. This filter is only applied in flow regions far away from solid boundaries. The time integration of the fluid equations is carried out by the fully implicit second-order scheme of Beam and Warming [13] in the near-wall region in order to overcome the time step restriction. A third-order Runge-Kutta scheme is used for time advancement of the equations in flow regions far away from solid boundaries. No-slip adiabatic wall boundary conditions are applied along the solid surfaces and characteristic plus sponge boundary conditions are applied in the far field locations. The numerical tool has been previously validated for several simulations of compressible flows involving sound generation and propagation [3, 4, 7].

3 ACOUSTIC PREDICTIONS

The acoustic predictions are performed by the FW-H acoustic analogy formulation [2]. The frequency domain formulation presented by [14] is implemented and incorporates convective effects. Surface dipole integrations are computed along the airfoil surface and a Hanning filter is applied in an energy preserving manner [14] to dipole sources before they are transformed to the frequency domain. Volume integrations of quadrupole source terms appearing in the FW-H equation are performed using the 3-D convective wideband multi-level adaptive fast multipole method (FMM) developed by [4, 15] to reduce the computational cost of the calculation of aeroacoustic integrals in the FW-H formulation.

4 RESULTS

This section discusses results obtained by DNC and the FW-H equation for the unsteady flow past a cylinder in the proximity of a NACA 0012 airfoil. The flow configurations investigated allow a study of sound generation due to interaction of boundary layers and wakes, including vortex shedding. The flow Reynolds numbers based on the airfoil chord and cylinder diameter are $Re_c = 5000$ and $Re_d = 200$, respectively. The freestream Mach numbers considered in the flow calculations and acoustic predictions are $M_\infty = 0.1, 0.3$ and 0.5 , and the angle of incidence is fixed at $AoA = 5$ deg. The present grid configuration consists of body-fitted O-grid blocks around airfoil and cylinder surfaces and a background O-grid block that resolves the acoustic far field. The airfoil grid block is composed of 400×60 grid points, in the periodic and wall normal directions, respectively, and the cylinder grid block is composed of 240×50 grid points, in the periodic and wall normal directions. These grid blocks are designed to accurately resolve the laminar boundary layers that develop along the airfoil and cylinder surfaces. The far field background grid block has 400×625 points, in the periodic and wall normal directions, respectively, with smooth stretching to accurately capture the sound radiation. In order to evaluate the effects of cylinder position on acoustic scattering and diffraction, the cylinder grid block is displaced from the half-chord position to the trailing edge position. A summary of the

flow configurations investigated is presented in Table 1. The airfoil has normalized chord $c = 1$ with trailing edge at $(x, y) = (1.0c, 0.0)$. Since the airfoil is at $AoA = 5$ deg, figures show the configuration rotated by -5 deg. All directivity plots in the paper are computed for a coordinate system located at the airfoil half-chord position.

Configuration	Freestream	
	Mach Number	Position of Cylinder Center (x,y)
1	0.1	Half-chord $(0.5c, 0.25c)$
2	0.3	Half-chord $(0.5c, 0.25c)$
3	0.5	Half-chord $(0.5c, 0.25c)$
4	0.1	Trailing edge $(1.0c, 0.25c)$
5	0.3	Trailing edge $(1.0c, 0.25c)$
6	0.5	Trailing edge $(1.0c, 0.25c)$

Table 1: Summary of flow configurations investigated.

Figure 1 presents the acoustic predictions for the cylinder vortex shedding frequency for case 1. Here, the cylinder is located above the airfoil half-chord and the freestream Mach number is $M_\infty = 0.1$. In Fig. 1 (a), one can see a detail view of the Fourier transformed acoustic field obtained by DNC. At the cylinder vortex shedding frequency, the Helmholtz number is given by $He = kc = 3.4$ and the equivalent Strouhal number is $St = fc/U_\infty = 5.4$. For this frequency, the acoustic field is composed by acoustic waves that are generated by the cylinder and are either reflected upwards by the airfoil surface or diffracted along the airfoil trailing edge. In Fig. 1 (b), one can observe a directivity plot of acoustic pressures obtained for the separate noise sources including the airfoil and cylinder dipoles and the volume quadrupoles. In the plot, observer positions are at $r = 5c$. As expected for such a low Mach number problem, acoustic radiation is dominated by dipole sources and quadrupole sources can be neglected in the far field acoustic prediction. Figure 1 (b) also shows that, for the present low frequency problem, the dipolar acoustic fields from airfoil and cylinder are similar to those expected from a free-field Green's function [16]. In the same figure, one can also see that both dipole sources present similar amplitudes in terms of sound radiation. Despite the fact that pressure amplitudes are similar for airfoil and cylinder dipoles, phase angles are shifted and there is a strong noise cancellation below the airfoil. This effect can be observed in Fig. 1 (c), when the total noise radiation is computed. In the same figure, one can see the good comparison in terms of acoustic pressure levels between the DNC and the FW-H solution.

In Figs. 2 and 3, one can observe the acoustic predictions for cases 2 and 3 at $M_\infty = 0.3$ and $M_\infty = 0.5$, respectively. Similarly to case 1, the cylinder is located above the airfoil half-chord. Figures 2 (a) and 3 (a) present the acoustic fields obtained by DNC for the cylinder vortex shedding frequency. For cases 2 and 3, the Helmholtz and Strouhal numbers are given by $He = 9.8$ and $St = 5.2$, and $He = 16.0$ and $St = 5.1$, respectively. Similarly to case 1, the acoustic fields for the present cases are composed by acoustic waves generated by the cylinder. However, scattering effects become more pronounced at higher Helmholtz numbers and, therefore, they considerably modify the acoustic fields. While acoustic waves are mainly reflected upwards for case 2, they are reflected in several directions for case 3. Diffraction effects along leading and trailing edges can also be observed in the figures for both cases.

Since, for the present configurations analyzed, the Helmholtz numbers are larger than 2π , the airfoil behaves as a non-compact body. Such effect can be observed in the acoustic directivity

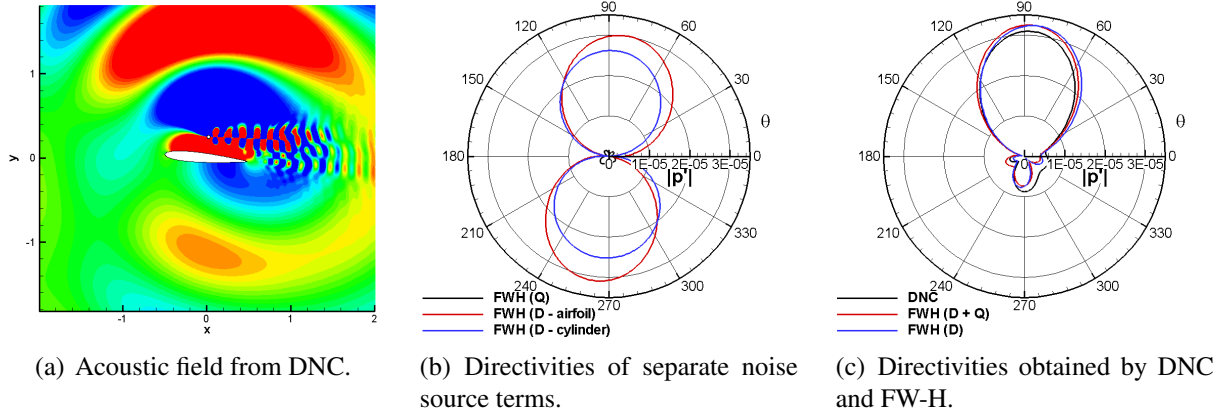


Figure 1: Acoustic predictions for $M_\infty = 0.1$, cylinder at half-chord position and results at the cylinder vortex shedding frequency.

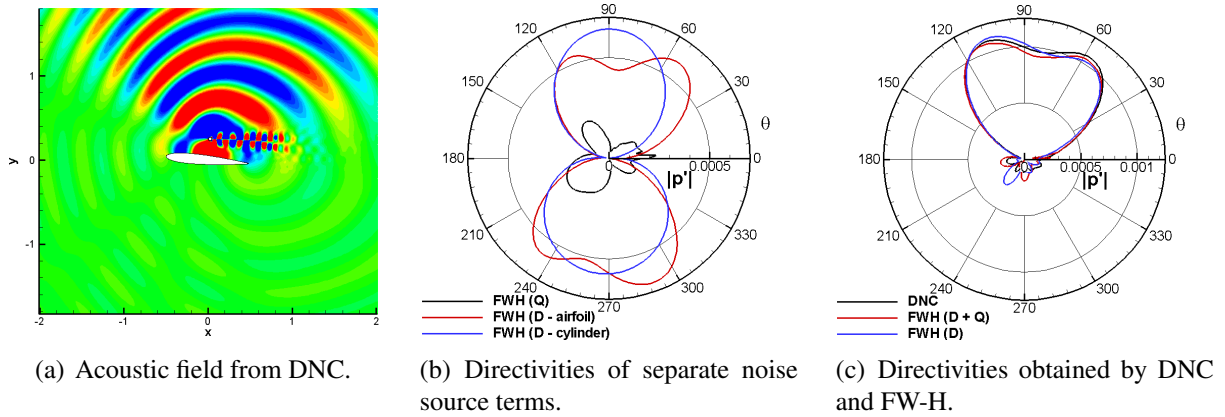


Figure 2: Acoustic predictions for $M_\infty = 0.3$, cylinder at half-chord position and results at the cylinder vortex shedding frequency.

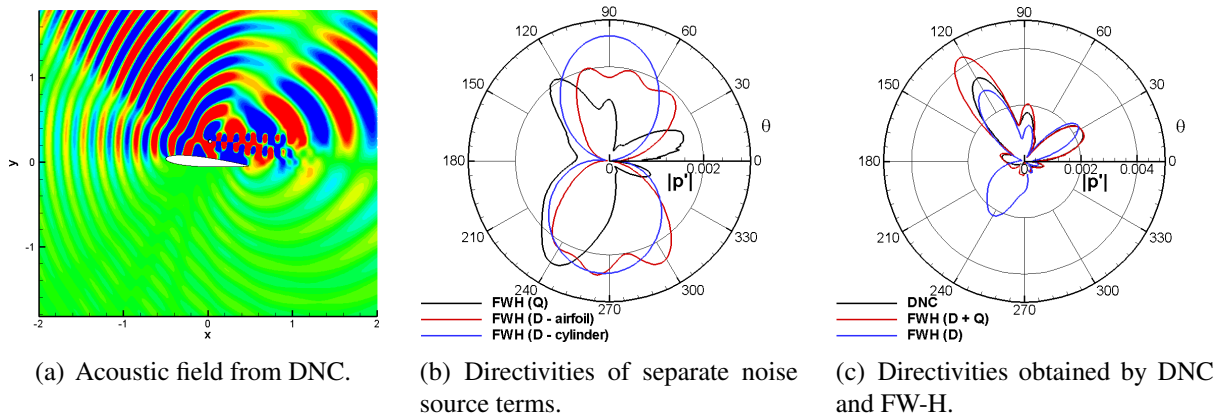


Figure 3: Acoustic predictions for $M_\infty = 0.5$, cylinder at half-chord position and results at the cylinder vortex shedding frequency.

plots of the separate noise sources, shown in Figs. 2 (b) and 3 (b). One can see in these plots that the airfoil dipole directivities computed at $r = 2c$ resemble those from a half-space Green's function [17]. Figures 2 (b) and 3 (b) present a comparison of acoustic pressure values from each separate noise source. One can see that quadrupole noise contribution becomes relevant for the present flow configurations at moderate Mach numbers. In Figs. 2 (c) and 3 (c), directivities

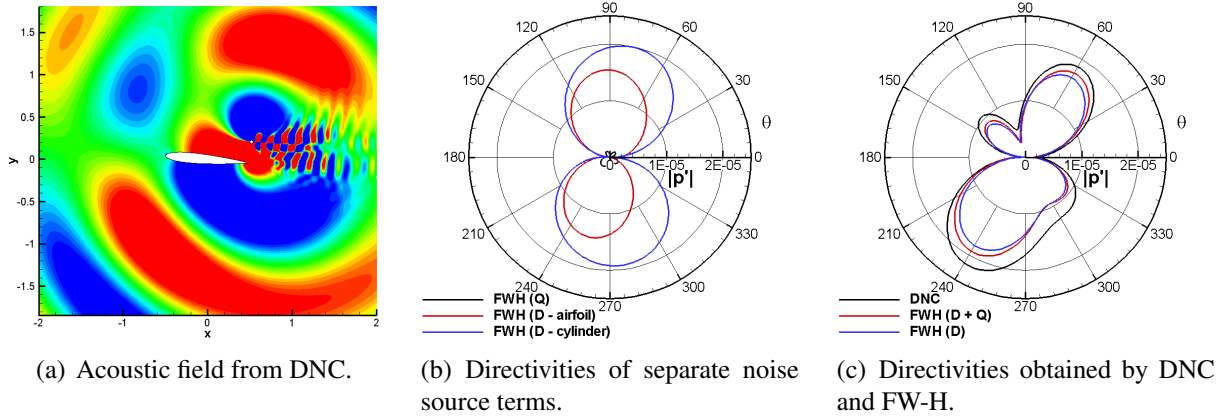


Figure 4: Acoustic predictions for $M_\infty = 0.1$, cylinder at trailing edge position and results at the cylinder vortex shedding frequency.

of total acoustic pressure obtained by DNC and the FW-H are shown. The latter are computed including the effects of dipoles without quadrupoles and the combined effects of dipoles and quadrupoles. The complex radiation patterns predicted using DNC are recovered by the FW-H formulation. In fact, the full directivity pattern for $M_\infty = 0.5$ is only accurately computed if quadrupole sources are added in the FW-H equation.

Figures 4 (a), (b) and (c) present the acoustic field, separate acoustic pressure directivities and total directivities computed by DNC and the FW-H equation at $r = 5c$, respectively, for case 4. Results shown in Fig. 4 are computed for the cylinder vortex shedding frequency with Helmholtz and Strouhal numbers given by $He = 3.2$ and $St = 5.1$, respectively. For the current flow configuration, the cylinder is positioned at the airfoil trailing edge and the freestream Mach number is $M_\infty = 0.1$. In Fig. 4 (a), one can observe that the acoustic field is similar to that of Fig. 1 (a). However, since the cylinder is displaced to the trailing edge region, acoustic diffraction is more pronounced for the present case. In Fig. 4 (b), one can notice that, for case 4, the amplitude of the airfoil dipole is smaller than that of the cylinder, differently from case 1. Such effect occurs since acoustic scattering along the airfoil surface is less intense. From the same figure, it is also possible to infer that quadrupole sources have negligible effect on total noise prediction for the current low Mach number. Figure 4 (c) shows the total acoustic directivity computed by DNC and the FW-H equation. While for case 1 most of the sound field was reflected upwards by the airfoil surface, for the present case, the sound field is more intense downwards, due to trailing edge diffraction.

In Figs. 5 and 6, one can observe results of acoustic predictions for case 5, for the airfoil and cylinder vortex shedding frequencies, respectively. These frequencies correspond to Helmholtz and Strouhal numbers equal to $He = 3.4$ and $St = 1.8$, and $He = 9.5$ and $St = 5.0$, respectively. It is possible to see in Figs. 5 (a), (b) and (c) that trailing edge scattering is the noise generation mechanism for the airfoil vortex shedding frequency. For such low frequency, quadrupole sources have a small contribution to far field radiation and the cylinder dipole can be neglected in the total noise prediction. The total acoustic directivity is typical of low frequency airfoil trailing edge noise [7].

Similarly to the results presented for case 4, results shown in Fig. 6 for the cylinder vortex shedding frequency of case 5 demonstrate that acoustic diffraction becomes more pronounced when the cylinder is displaced towards the trailing edge. However, scattering effects are still dominant in terms of total noise radiation for the current case. From visualization of Figs. 6 (b) and (c), one can argue that, for the present flow configuration, acoustic scattering occurs

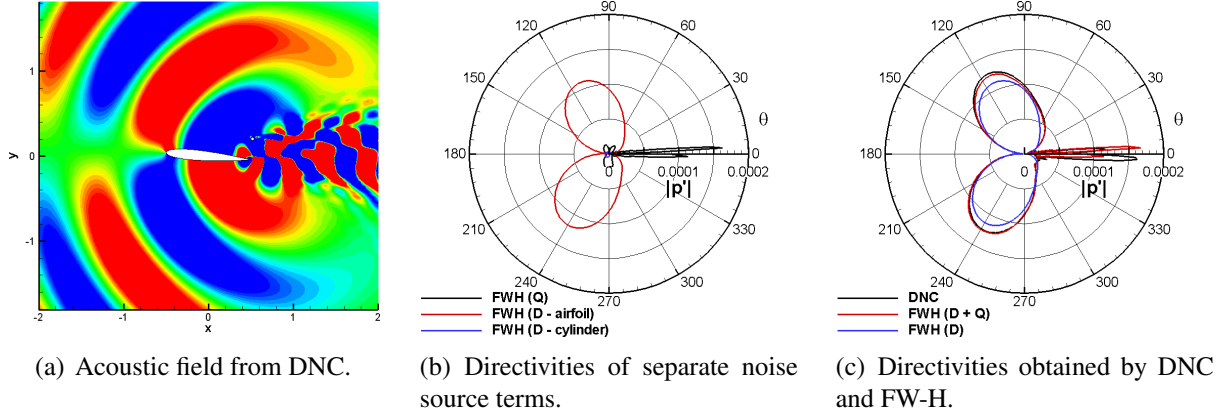


Figure 5: Acoustic predictions for $M_\infty = 0.3$, cylinder at trailing edge position and results at the airfoil vortex shedding frequency.

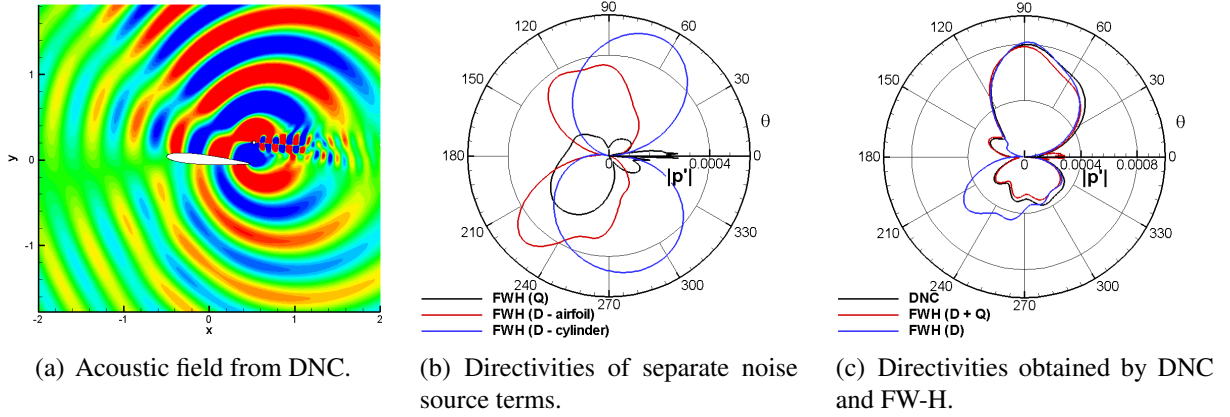


Figure 6: Acoustic predictions for $M_\infty = 0.3$, cylinder at trailing edge position and results at the cylinder vortex shedding frequency.

due to interaction of dipole sources, and diffraction effects can only be accurately predicted if quadrupole sources are included in the FW-H equation.

Figures 7 and 8 present acoustic prediction results of case 6 for the airfoil and cylinder vortex shedding frequencies, respectively. These frequencies correspond to Helmholtz and Strouhal numbers equal to $He = 5.5$ and $St = 1.8$, and $He = 15.3$ and $St = 4.9$, respectively. Directivity plots are obtained for observer positions at $r = 2c$. Similarly to Fig. 3 (a), in Figs. 7 (a) and 8 (a), one can observe the complex patterns of the radiated fields, composed by the incident acoustic field due to the quadrupole sources and the scattered field due to the dipole sources. Figures 7 (b) and (c) show that, for the airfoil vortex shedding frequency, the total noise radiation is obtained by the sum of sound fields from quadrupole and airfoil dipole sources. As previously observed for case 5, the far field noise contribution of the cylinder dipole is negligible at this frequency.

In Ref. [7], the authors demonstrate that quadrupole sources are only relevant for acoustic predictions of moderate Mach number flows at high frequencies. The present results indicate that, even at low frequencies, quadrupole sources are of paramount importance for the total noise prediction of a moderate Mach number flow with wake interaction. In Figs. 7 (c) and 8 (c), one can see that the noise predictions obtained by the FH-W formulation show excellent agreement with those obtained by DNC when quadrupoles are taken into account. In the latter figure, and also from Fig. 8 (b), for the cylinder vortex shedding frequency, one can claim

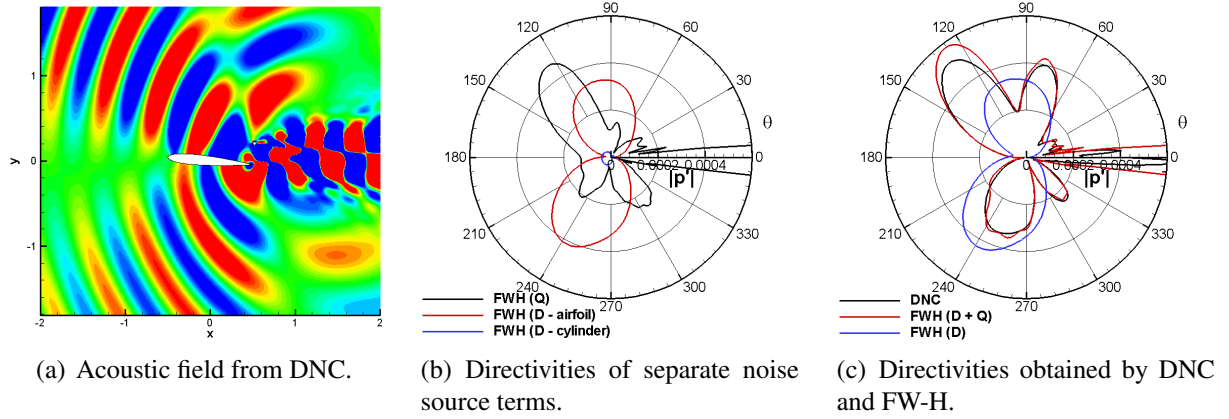


Figure 7: Acoustic predictions for $M_\infty = 0.5$, cylinder at trailing edge position and results at the airfoil vortex shedding frequency.

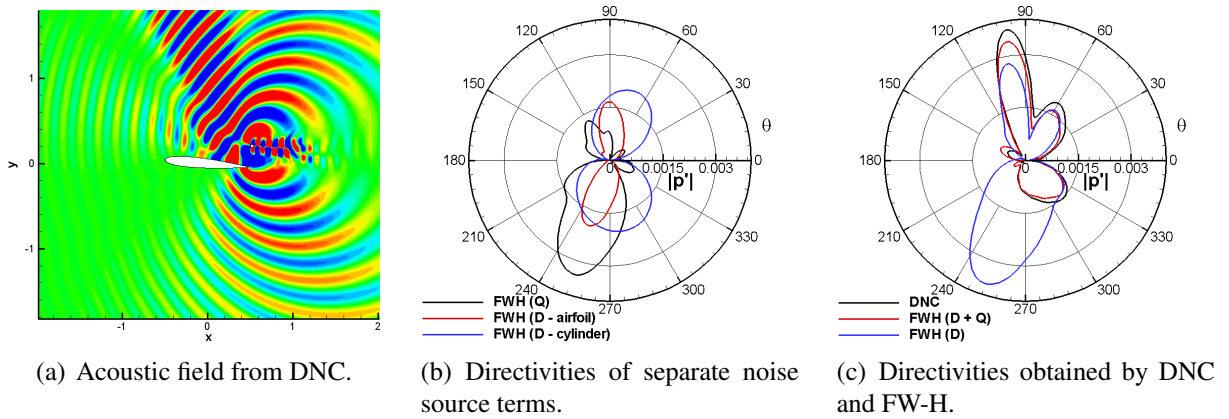


Figure 8: Acoustic predictions for $M_\infty = 0.5$, cylinder at trailing edge position and results at the cylinder vortex shedding frequency.

that quadrupole sources are more directly related to the acoustic diffraction phenomenon that occurs at the airfoil trailing edge. Therefore, for the present moderate Mach number, if the airfoil vortex shedding is the driving noise source mechanism, quadrupole and dipole sources are related to incident far field noise radiation. However, if the cylinder vortex shedding is the driving noise source mechanism, quadrupole sources are more related to diffraction effects and dipole sources are related to both scattering and diffraction phenomena.

5 CONCLUSIONS

The work here reported has presented aeroacoustic predictions of a model airframe noise problem. The effort was conducted in order to assess the effects of wake and boundary layer interaction on both the flow and acoustic fields. Hence, simulations of unsteady laminar flows are performed for a two-dimensional configuration composed of a cylinder placed above a NACA 0012 airfoil at 5 deg. angle of incidence. Such calculations include both noise generation and its subsequent propagation to the far field. For all test cases, the Reynolds number based on the airfoil chord is set at $Re_c = 5000$ and the Reynolds number based on the diameter of the cylinder is $Re_d = 200$. The work performs an assessment of cylinder position and freestream Mach number effects on sound radiation for $M_\infty = 0.1, 0.3$ and 0.5 . The investigation of the noise sources for airfoil and cylinder vortex shedding frequencies is also presented using a hy-

brid methodology which employs direct calculation for near field source computations and the Ffowcs Williams-Hawkings (FW-H) equation as the acoustic analogy formulation. In order to verify the numerical solutions, acoustic prediction results obtained by direct noise calculation (DNC) are compared to those computed by the FW-H equation and good agreement is observed.

The results indicate that, when the cylinder vortex shedding is the driving noise source mechanism, intense dipolar interference occurs for all configurations analyzed. When the cylinder is positioned at half-chord location, acoustic scattering along the airfoil surface is more pronounced and dipolar interference is constructive above the airfoil, increasing noise radiation upwards. Underneath the airfoil, dipole sources are out of phase and noise radiation is reduced in that direction. When the cylinder is located above the trailing edge, dipolar interference presents more complicated patterns with combined diffraction and scattering effects. It is found that while quadrupole sources can be neglected in noise predictions by the FW-H equation for the $M_\infty = 0.1$ flow calculations, they should be included for the $M_\infty = 0.3$ and 0.5 acoustic predictions at low and high frequencies.

For moderate Mach number flows, at the cylinder vortex shedding frequency, dipole sources are related to both acoustic scattering and diffraction phenomena that occur along the airfoil surface and trailing edge, respectively. However, quadrupole sources are more specifically related to diffraction effects along the airfoil trailing edge. Good general agreement between DNC and noise predictions obtained by acoustic analogy are observed for all test cases analyzed. However, small differences can be noticed in a comparison of pressure directivities, specially for $M_\infty = 0.5$. These differences can be caused by non-uniform flow effects on noise radiation. While DNC includes these effects in the computations, the current implementation of the FW-H assumes radiation in the presence of a uniform mean flow. This topic should be investigated in future research.

ACKNOWLEDGEMENTS

The authors acknowledge the partial financial support received from Fundação de Amparo à Pesquisa do Estado de São Paulo, FAPESP, under Grants No. 2011/12493-6, No. 2013/03508-5 and No. 2013/07375-0. The partial support received from Conselho Nacional de Desenvolvimento Científico e Tecnológico, CNPq, under Grants No. 312064/2006-3 and No. 471592/2011-0 is also gratefully acknowledged. The authors are also indebted to the PIBIC Scholarships No. 145126/2012 and No. 142972/2012-6 provided by CNPq to the second and third authors, respectively.

REFERENCES

- [1] M.J. Lighthill, On sound generated aerodynamically I. General theory. *Proceedings of the Royal Society A*, **211**, 564–587, 1952.
- [2] J.E. Ffowcs Williams and D.L. Hawkings, Sound generation by turbulence and surface in arbitrary motion. *Philosophical Transaction of the Royal Society of London, Series A, Mathematical and Physical Sciences*, **264**, 321–342, 1969.
- [3] W.R. Wolf and S.K. Lele, Acoustic analogy formulations accelerated by fast multipole method for two-dimensional aeroacoustic problems. *AIAA Journal*, **48**, 2274–2285, 2010.
- [4] W.R. Wolf and S.K. Lele, Aeroacoustic integrals accelerated by fast multipole method. *AIAA Journal*, **49**, 1466–1477, 2011.

- [5] J.H. Casper, D.P. Lockard, M.R. Khorrami, and C.L. Streett, Investigation of volumetric sources in airframe noise simulations. AIAA Paper No. 2004-2805, *Proceedings of the 10th AIAA/CEAS Aeroacoustics Conference*, 2004.
- [6] P.R. Spalart, M.L. Shur, M.K. Strelets, and A.K. Travin, Towards noise prediction for rudimentary landing gear. *IUTAM Symposium on Computational Aeroacoustics for Aircraft Noise Prediction*, 2010.
- [7] W.R. Wolf, J.L.F. Azevedo, and S.K. Lele, Convective effects and the role of quadrupole sources for aerofoil aeroacoustics. *Journal of Fluid Mechanics*, **708**, 502–538, 2012.
- [8] W.R. Wolf, J.L.F. Azevedo, and S.K. Lele, Effects of mean flow convection and quadrupole sources on airfoil trailing edge noise. AIAA Paper No. 2012-2056, *Proceedings of the 18th AIAA/CEAS Aeroacoustics Conference*, AIAA, Colorado Springs, Colorado, 2012.
- [9] C. Yu, W.R. Wolf, and S.K. Lele, Quadrupole noise in turbulent wake interaction problems. AIAA Paper No. 2012-2057, *Proceedings of the 18th AIAA/CEAS Aeroacoustics Conference*, AIAA, Colorado Springs, Colorado, 2012.
- [10] S. Nagarajan, S.K. Lele, and J.H. Ferziger, A robust high-order method for large eddy simulation. *Journal of Computational Physics*, **191**, 392–419, 2003.
- [11] R. Bhaskaran and S.K. Lele, Large eddy simulation of free-stream turbulence effects on heat transfer to a high-pressure turbine cascade. *Journal of Turbulence*, **11**, 1–15, 2010.
- [12] S.K. Lele, Compact finite difference schemes with spectral-like resolution. *Journal of Computational Physics*, **103**, 16–42, 1992.
- [13] R.M. Beam and R.F. Warming, An implicit factored scheme for the compressible Navier-Stokes equations. *AIAA Journal*, **16**, 393–402, 1978.
- [14] D.P. Lockard, An efficient, two-dimensional implementation of the Ffowcs Williams and Hawkins equation. *Journal of Sound and Vibration*, **229**, 897–911, 2000.
- [15] W.R. Wolf and S.K. Lele, Wideband fast multipole boundary element method: Application to acoustic scattering from aerodynamic bodies. *International Journal for Numerical Methods in Fluids*, **67**, 2108–2129, 2011.
- [16] N. Curle, The influence of solid boundaries upon aerodynamic sound. *Proceedings of the Royal Society A*, **231**, 505–514, 1955.
- [17] J.E. Ffowcs Williams and L.H. Hall, Aerodynamic sound generation by turbulent flow in the vicinity of a scattering half plane. *Journal of Fluid Mechanics*, **40**, 657–670, 1970.